Author/s:
Bastin, G;Nešić, D;Tan, Y;Mareels, I

Title:
On extremum seeking in bioprocesses with multivalued cost functions

Date:
2009-05-01

Citation:
Bastin, G., Nešić, D., Tan, Y. & Mareels, I. (2009). On extremum seeking in bioprocesses with multivalued cost functions. Biotechnology Progress, 25 (3), pp.683-689. https://doi.org/10.1002/btpr.87.

Persistent Link:
https://hdl.handle.net/11343/299534

On Extremum Seeking in Bioprocesses with Multivalued Cost Functions*

Georges Bastin†, Dragan Nešić‡, Ying Tan‡ and Iven Mareels‡

July 18, 2008

Abstract

Finding optimal operating modes for bioprocesses has been, for a long time, a relevant issue in bioengineering. The problem is of special interest when it implies the simultaneous optimization of competing objectives. In this paper we address the problem of finding optimal steady-states that achieve the best trade off between yield and productivity by using non-model based extremum-seeking control with semi-global practical stability and convergence properties. A special attention is paid to processes with multiple steady-states and multivalued cost functions.

1 Introduction

Finding optimal operating modes for bioprocesses has been, for a long time, a relevant issue in bioengineering. The problem is of special interest when it implies the simultaneous optimization of competing objectives. This situation arises in particular in many continuous or fed-batch bioprocesses that are characterized by a conflict between the yield and the productivity. Under the assumption that a kinetic model of the process is known to the user, the problem of finding steady-states or operating modes that achieve the best trade off between yield and productivity has been addressed for instance by Modak and Lim [8]-[9], by Shimizu [10] and by Jadot et al. [5].

In this paper we address the issue of optimizing bioreactors by using so-called "Extremum Seeking (ES)" techniques. A non-model based approach to extremum seeking for bioreactors was first intitiated by Wang et al. in [14]. An alternative model-based approach was then pursued in a series of papers by Guay and several co-workers in e.g. [6], [7], [15].

Here we follow the non-model based approach. We assume that neither the process kinetics nor the cost function are known to the user. It is just assumed that the numerical value of the cost is obtained on-line from process measurements. We want to examine how the automatic seeking of an optimal steady state can be achieved by using non-model based extremum-seeking control, especially in the case where the cost function is a multivalued function.

Our paper is organized as follows. First in Section 2, we provide a self-content characterization of the steady-states that achieve an optimal trade-off between yield and productivity maximization in biochemical processes. Then, in Section 3, we show how this optimization problem can be solved by using a novel feedback extremum seeking scheme with semi-global stability and convergence

*This work was supported by the Belgian Programme on Interuniversity Attraction Poles (IAP V/22) and by National ICT Australia (NICTA).

†Center for Systems Engineering and Applied Mechanics, Department of Mathematical Engineering, Université Catholique de Louvain, 4, avenue G. Lemaitre, 1348 Louvain-la-Neuve, Belgium.

‡The Department of Electrical and Electronics Engineering, University of Melbourne, Melbourne, Vic 3010, Australia.

properties. This novel ES scheme has been proposed in a recent paper by Tan et al. [11] and is simpler than the original scheme which was used in [14] (see also the book [1], Chapter 8). Furthermore, instead of using linearisation about the equilibrium to prove local stability as in [14], the method of [11] allows to analyse the semi-global stability of the system. Then, our main contribution is in Sections 4 and 5 where we show how the semi-global stability analysis of [11] can be exploited to address situations with multiple steady-states and a multivalued cost function by using generalized singular perturbation results as presented, for example, in [13]. In this analysis, the Aumann integral [2] is used to define the average of all possible behaviors of the slow system and as a result the average of the slow system is a differential inclusion. We consider the very simplest case where the cost is a multivalued function and we demonstrate a new phenomenon where the system trajectory is stuck in a non-extremum bifurcation point. Then we propose a way to overcome this difficulty and we provide a theoretical sketch of the analysis of its efficiency. We believe that viewing the problem in this manner is novel and could lead to solutions of various other problems not considered in this paper.

For the sake of simplicity and clarity, we limit ourselves to processes where a single monomolecular irreversible reaction takes place. However, even though we deal only with the simplest possible situation, the issues that emerge from our analysis are relevant for more general situations involving multi-molecular enzymatic reactions or cell growth reactions as in [14].

2 Yield-Productivity tradeoff

The objective of this preliminary section is to give a characterisation of the steady-states that achieve an optimal trade-off between yield and productivity maximization in biochemical processes. We present the very simplest case where a conflict between yield and productivity may occur. We consider a single irreversible enzymatic reaction of the form:

$$\mathbf{X}_1 \longrightarrow \mathbf{X}_2$$

with $\mathbf{X}_1$ the substrate (or reactant) and $\mathbf{X}_2$ the product. The reaction takes place in the liquid phase in a continuous stirred tank reactor. The substrate is fed into the reactor with a constant concentration c at a volumetric flow rate u. The reaction medium is withdrawn at the same volumetric flow rate u so that the liquid volume V is kept constant. The process dynamics are described by the following standard mass-balance state space model:

$$\dot{x}_1 = -r(x_1) + (u/V)(c - x_1) \tag{1a}$$

$$\dot{x}_2 = r(x_1) - (u/V)x_2 \tag{1b}$$

where x_1 is the substrate concentration, x_2 is the product concentration and $r(x_1)$ is the reaction rate (called *kinetics*). Obviously this system makes physical sense only in the non-negative orthant $x_1 \geqslant 0$, $x_2 \geqslant 0$. Moreover the flow rate u (which is the control input) is non-negative by definition and physically upper-bounded (by the feeding pump capacity):

$$0 \leqslant u \leqslant u^{max}. \tag{2}$$

In this paper we shall investigate two different cases depending on the form of the rate function $r(x_1)$. We begin with Michaelis-Menten kinetics which is the most basic model for enzymatic reactions (e.g. [3, Chapter 4]) :

$$r(x_1) = \frac{v_m x_1}{K_m + x_1}$$

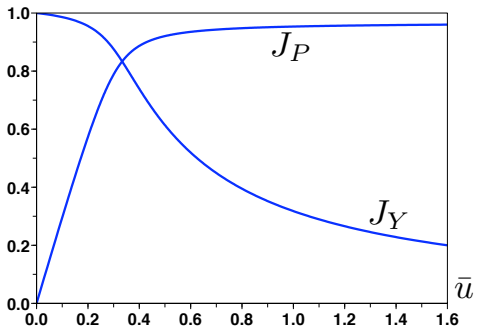

Figure 1: Productivity J_P and yield J_Y for system (3) with $c = 3$ and $K_m = 0.1$.

with v_m the maximal reaction rate and K_m the half-saturation constant. To normalise the model we use $v_m V$ and v_m^{-1} as the units of u and time respectively. So the normalised model becomes

$$\dot{x}_1 = -\frac{x_1}{K_m + x_1} + u(c - x_1) \tag{3a}$$

$$\dot{x}_2 = \frac{x_1}{K_m + x_1} - ux_2. \tag{3b}$$

It can be readily verified that, for any positive constant input flow rate $\bar{u} \in (0, u^{max}]$, there is a unique steady-state $\bar{x}_1 = \varphi_1(\bar{u})$, $\bar{x}_2 = \varphi_2(\bar{u})$ solution of the following equations:

$$\bar{x}_1 + \bar{u}(c - \bar{x}_1)(K_m + \bar{x}_1) = 0 \tag{4a}$$

$$(c - \bar{x}_2) - \bar{u}\bar{x}_2(K_m + c - \bar{x}_2) = 0. \tag{4b}$$

Furthermore each admissible steady-state belongs to the set

$$\Omega = \{(\bar{x}_1, \bar{x}_2) : \bar{x}_1 \geqslant 0, \bar{x}_2 \geqslant 0, \bar{x}_1 + \bar{x}_2 = c\}$$

and is globally asymptotically stable in the non-negative orthant.

The industrial objective of the process is the production of the reaction product. For process optimization, two steady-state performance criteria are considered : the *productivity* J_P and the *yield* J_Y. The productivity is the amount of product harvested in the outflow per unit of time :

$$J_P = \bar{u}\bar{x}_2 = \bar{u}\varphi_2(\bar{u})$$

The yield is the amount of product made per unit of substrate fed to the reactor:

$$J_Y = \frac{\bar{x}_2}{c} = \frac{\varphi_2(\bar{u})}{c}$$

The sensitivity of J_P and J_Y with respect to $\bar{u}$ is illustrated in Fig. 1. A conflict between yield and productivity is clearly apparent: the productivity J_P is an increasing function (from 0 to 100%) of $\bar{u}$ while the yield J_Y is decreasing (from 100 to 0%). Operating the process at a yield J_Y close to 100% can result in a dramatic decrease of the productivity J_P (and vice-versa): it does not really make sense to optimize one of the criteria disregarding the other one. The process must be operated at a steady-state that achieves a trade-off between yield and productivity. This is

typically a "multicriteria" optimization problem since the two criteria are antagonistic. A standard way to address the problem is to define an overall performance index as a convex combination of J_P and J_Y:

$$J_T(\bar{u}) \triangleq \lambda J_P + (1-\lambda) J_Y = \varphi_2(\bar{u}) \left[\lambda \bar{u} + \frac{1-\lambda}{c} \right] \qquad \lambda \in [0,1]. \tag{5}$$

This cost function is illustrated in Fig. 2 where it is readily seen that it has a unique global maximum u^*. The corresponding optimal steady-state is naturally defined as $x_1^* = \varphi_1(u^*)$, $x_2^* = \varphi_2(u^*)$.

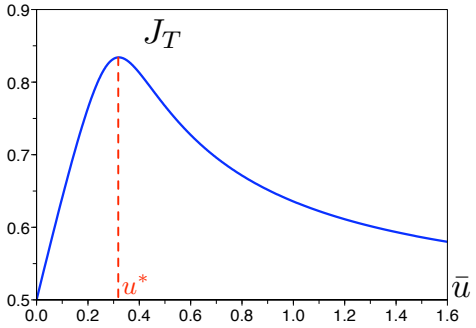

Figure 2: Overall performance index J_T for system (3) with $c = 3$, $K_m = 0.1$ and $\lambda = 0.5$.

3 Extremum seeking control

Our concern is to design a non-model based ES feedback controller able to automatically drive the process to the optimal operating point (x_1^*, x_2^*) that maximizes J_T without any precise knowledge of u^*. It is assumed that the process is equipped with an on-line sensor that measures the product concentration x_2 in the outflow. We then define a scalar ES scheme of the form proposed in [11]:

$$y(t) = \lambda u(t) x_2(t) + (1-\lambda)\frac{x_2(t)}{c} \tag{6a}$$

$$d(t) = a \sin(\omega t) \tag{6b}$$

$$\dot{\theta}_0(t) = k\omega y(t) d(t) \tag{6c}$$

$$\theta(t) = \theta_0(t) + d(t) \tag{6d}$$

$$u(t) = \alpha(\theta(t)) \tag{6e}$$

where $u = \alpha(\theta)$ is a smooth sigmoid function as depicted in Fig. 3 while (a, k, ω) are positive tuning parameters. In this feedback control law, the exogenous signal $d(t)$ is a so-called *dither* that activates the extremum seeking and can be any periodic function of time. Here we work with a sinusoidal dither $d(t) = a \sin(\omega t)$.

In order to avoid any confusion, it must be stressed here that the ES algorithm (6) is a genuine non-model based control algorithm. This means that the controller needs no knowledge of the model (it does not involve any kind of explicit or implicit internal model of the process). From the controller viewpoint, the plant is a black box whose input can be manipulated and output is measured. In particular, as we have mentioned in the Introduction, the kinetic rate function $r(x_1)$, the dynamical model (1) and the function $J_T(\bar{u})$ are unknown to the user and do not appear in

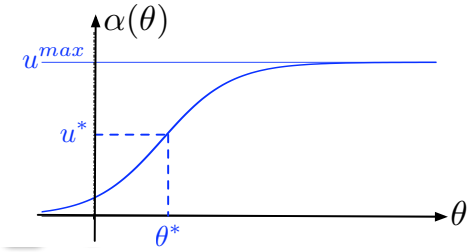

Figure 3: Sigmoid function $\alpha(\theta)$.

the control scheme (6). More precisely, we can say that the user has decided to maximise the composite cost $J_T = \lambda u x_2 + (1-\lambda)c^{-1}x_2$ but he does not know that J_T is a function of $\bar{u}$ of the form (5) shown in Fig.2. The rationale behind the control law is to use on-line measurements of x_2 to progressively learn the shape of the cost function and try to climb up to the top by adjusting the input u.

But, obviously, we may use the model (1) as a benchmark process for testing the feasibility and the efficiency of the proposed ES algorithm in simulations. In Fig. 4 the operation of the ES control algorithm (6) is illustrated for appropriately tuned parameters $a = 0.02$, $k = 1$, $\omega = 0.1$. We see that there is a time scale separation between the system itself and the climbing mechanism. Starting from an initial condition $(x_1(0), x_2(0))$, there is first a fast convergence of the state to the nearest (stable) steady-state which is followed by a slow quasi-static climbing along the cost function up to the maximum. This behaviour is guaranteed from any initial condition so that we have the following semi-global convergence property.

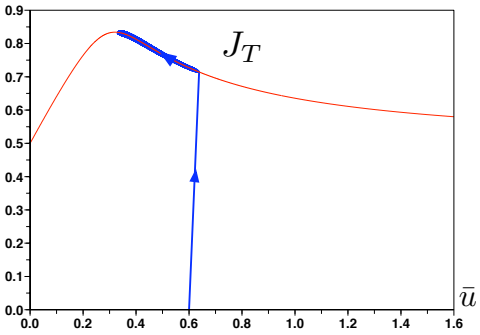

Figure 4: Extremum seeking for system (3) with $a = 0.02$, $k = 1$, $\omega = 0.1$.

Property 1. For any initial condition $(x_1(0) \geqslant 0, x_2(0) \geqslant 0, \theta_0(0))$ and for any $\nu > 0$, there exist parameters (a, k, ω) such that, for the closed-loop system (3)-(6), $x_1(t) \geqslant 0$, $x_2(t) \geqslant 0$, $\theta_0(t)$ bounded and

$$\limsup_{t\to\infty} \Big(|x_1(t) - x_1^*| + |x_2(t) - x_2^*| + |u(t) - u^*| \Big) \leqslant \nu.$$

This property[1] obviously implies that $\limsup_{t\to\infty} |y(t) - J_T(u^*)|$ can be made arbitrarily small:

[1] Actually a stronger property can be shown to hold : For any compact set of initial conditions the parameters (a,

from any initial condition, the output $y(t)$ can be driven and regulated arbitrarily close to the optimal performance value $y^* = J_T(u^*)$.

Property 1 is a straightforward consequence of Theorem 1 in [11] which notably involves a singular perturbation and an averaging Lyapunov stability analysis that can be summarized in the following way. From (4), for each $\theta \in \mathbb{R}$, the system (3) with input $\bar{u} = \alpha(\theta)$ has a single equilibrium $\bar{x}_1 = \varphi_1(\alpha(\theta)), \bar{x}_2 = \varphi_2(\alpha(\theta))$ which is globally asymptotically stable. The cost function J_T can then be viewed as a function of θ expressed as

$$J_T = Q(\theta) = \left[\lambda\alpha(\theta) + \frac{(1-\lambda)}{c}\right]\varphi_2(\alpha(\theta)).$$

This function is convex and has a unique global maximum at $\theta^* = \alpha^{-1}(u^*)$ with the property that

$$Q'(\theta^* + \zeta)\zeta < 0 \quad \forall \zeta \neq 0. \tag{7}$$

The change of variables $\tilde{\theta} \triangleq \theta_0 - \theta^*$ and the change of time scale $\sigma \triangleq \omega t$ are introduced. Then, the "slow" θ_0-dynamics (6c) along the static characteristic $\bar{x}_1 = \varphi_1(\alpha(\theta)), \bar{x}_2 = \varphi_2(\alpha(\theta))$ are rewritten as

$$\frac{d\tilde{\theta}}{d\sigma} = kQ(\theta^* + \tilde{\theta} + a\sin\sigma)a\sin\sigma. \tag{8}$$

Applying a Taylor series expansion, this equation is rewritten as

$$\frac{d\tilde{\theta}}{d\sigma} = ka\left[f(\sigma,\tilde{\theta}) + a^2 R\right]$$

whith $f(\sigma,\tilde{\theta}) \triangleq Q(\theta^* + \tilde{\theta})\sin\sigma + aQ'(\theta^* + \tilde{\theta})\sin^2\sigma$ and R contains higher order terms in $\sin\sigma$. The function $f(\sigma,\tilde{\theta})$ being 2π-periodic in σ, if the parameter a is taken small enough, we can neglect the higher order terms and we have for the averaged system

$$\frac{d\theta_{av}}{d\sigma} = ka\frac{1}{2\pi}\int_0^{2\pi} f(\sigma,\theta_{av})d\sigma \triangleq \frac{ka^2}{2}Q'(\theta^* + \theta_{av}).$$

This system is globally asymptotically stable as can be seen from the Lyapunov function $V = (1/2)\theta_{av}^2$, since

$$\frac{dV}{d\sigma} = \frac{ka^2}{2}Q'(\theta^* + \theta_{av})\theta_{av} < 0 \quad \forall\theta_{av} \neq 0$$

because of condition (7).

The case-study that we have presented so far is representative of biochemical processes that exhibit some yield-productivity decoupling as observed in many practical applications (see e.g. [5] or [10]). However it must be emphasized that Proposition 1 is restricted to situations where the two following conditions hold:

C1. For each admissible value of the flow rate $\bar{u}$ the system must have a single globally asymptotically stable equilibrium.

C2. The performance cost function must be single-valued and "well-shaped" in the sense that, for the admissible range of flow rate values $0 \leqslant \bar{u} \leqslant u^{max}$, it must have a single maximum value $J_T(u^*)$ without any other local extrema.

There are situations where these conditions are not satisfied: the system may have multiple (stable and unstable) equilibria for some input values $\bar{u}$ and the yield or productivity criteria may be multivalued functions. As we shall discuss in the next section, the problem may happen even with simple monomolecular reactions when the kinetics are subject to substrate inhibition or auto-catalytic effects (e.g. [14]).

---

k, ω) can be selected such that boundedness and convergence holds uniformly on the compact set of initial conditions (see [11] for details).

4 Multivalued performance cost function

We consider again the simple model (1) but we now assume that, in addition to the Michaelis-Menten kinetics, the reaction rate is subject to exponential substrate inhibition. The rate function is as follows:

$$r(x_1) = \frac{v_m x_1}{K_m + x_1} e^{-bx_1^p}$$

where b and p are two positive constant parameters. The dynamical model is written:

$$\dot{x}_1 = -\frac{v_m x_1}{K_m + x_1} e^{-bx_1^p} + u(c - x_1) \tag{9a}$$

$$\dot{x}_2 = \frac{v_m x_1}{K_m + x_1} e^{-bx_1^p} - ux_2 \tag{9b}$$

Depending on the value of $\bar{u} \in (0, u^{max}]$, the system may have one, two or three steady-states $(\bar{x}_1, \bar{x}_2)$ with $\bar{x}_1$ solution of:

$$\frac{v_m \bar{x}_1}{K_m + \bar{x}_1} e^{-b\bar{x}_1^p} = \bar{u}(c - \bar{x}_1)$$

and $\bar{x}_2 = c - \bar{x}_1$.

The productvity $J_P = \bar{u}\bar{x}_2$ is represented in Fig. 5 as a function of $\bar{u}$. In this example, J_P is clearly a multivalued function of $\bar{u}$. However it can be seen that it has a unique global maximum for $\bar{u} = u^*$. Moreover, the graph of Fig. 5 can also be regarded as a bifurcation diagram with

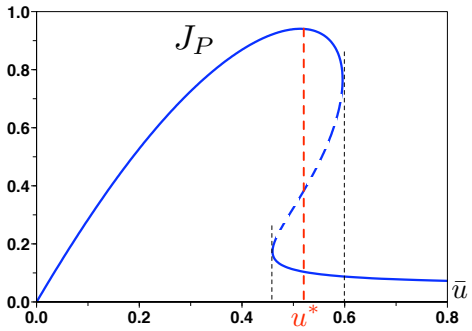

Figure 5: Productivity J_P for system (9) with $c = 3$, $v_m = 2$, $K_m = 1$, $b = 0.08$, $p = 3.4$.

respect to the parameter $\bar{u}$ where the solid branches correspond to stable equilibria and the dashed branch to unstable equilibria. Hence it can be seen that the maximum point is located on a stable branch.

Here we assume that the industrial objective is to achieve the maximization of the productivity J_P. Although conditions C1 and C2 are not satisfied in this case, a fully satisfactory operation of the ES control law (6) (with $y(t) = u(t)x_2(t)$) can nevertheless be observed in Fig. 6 and Fig. 7.

The result of Fig.6 is expected since we are in conditions quite similar to the previous case of Section 3. The result of Fig. 8 is more informative since here the convergence towards the maximum of the cost function is operated in two successive stages. In a first stage, there is a fast convergence to the nearest stable state which is located *on the lower stable branch* followed by a

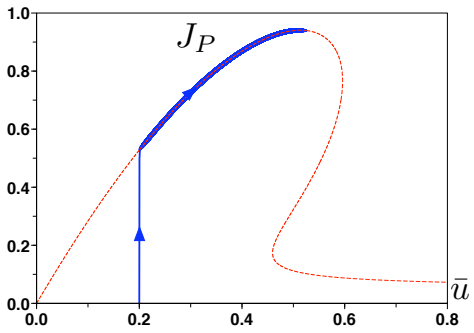

Figure 6: Extremum seeking for system (9) with $a = 0.003$, $k = 10$, $\omega = 0.01$.

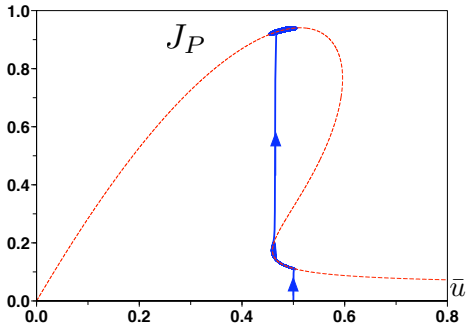

Figure 7: Extremum seeking for system (9) with $a = 0.003$, $k = 6$, $\omega = 0.01$.

quasi-steady-state progression along that branch. Then, when the state reaches the bifurcation point, there is a fast jump up to the *good upper branch* and a final climbing up to the maximum point. It is very important to emphasize here that, in order to get the result of Fig.7, the amplitude a of the dither signal must be large enough. Otherwise, the trajectory of the closed loop system definitely remains stuck on the lower branch at the bifurcation point as shown in Fig.8. On the other side, too large values of the dither amplitude are also prohibited because they produce cyclic trajectories as shown in Fig.9. From all these observations, we can conclude that by tuning the amplitude of the dither signal properly, it is possible to pass through the discontinuities of the stable branches of the cost function and to converge to the global maximum.

In the next section, we shall examine how the averaging Lyapunov stability analysis can be extended to the case of a multivalued (or "set-valued") cost function, by using the notion of "Integral of a set-valued function" ([2]). This analysis will explain why, in contrast with the previous case, it may be required to increase the parameter a for guaranteeing the convergence of the averaged system.

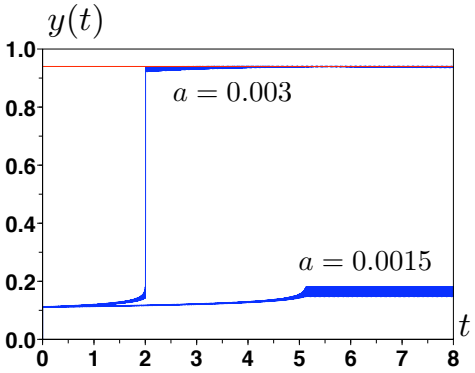

Figure 8: Output signal $y(t)$: when a is too small, the trajectory is stuck on the lower branch.

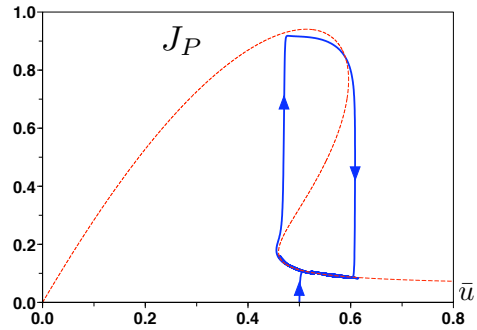

Figure 9: Extremum seeking for system (9) with $a = 0.015$, $k = 6$, $\omega = 0.01$.

5 Averaging stability analysis

In this section, we are concerned with the analysis of a dynamical system

$$\dot{x} = f(x, u) \tag{10a}$$

$$y = h(x, u) \tag{10b}$$

under the ES control law (6) whith a set-valued cost function having a form similar to Fig.5 (obviously we have system (9) in mind). Since only the stable branches of the static characteristic matter, the set-valued cost function $Q(\theta)$ is defined as a set of two continuous single-valued functions:

$$Q(\theta) = \{Q_1(\theta), Q_2(\theta)\}$$

with the following conditions:

1. $Q_1 : [\theta_1, +\infty) \to \mathbb{R}$ and $Q_2 : (-\infty, \theta_2] \to \mathbb{R}$ with $\theta_1 < \theta_2$;
2. For each value of $\theta \in [\theta_1, +\infty)$, there is a LAS equilibrium $x = \ell_1(\theta)$ of system (10) such that $Q_1(\theta) = h(\ell_1(\theta), \alpha(\theta))$;
3. For each value of $\theta \in (-\infty, \theta_2]$, there is a LAS equilibrium $x = \ell_2(\theta)$ of system (10) such that $Q_2(\theta) = h(\ell_2(\theta), \alpha(\theta))$;

4. $\forall \theta \in [\theta_1, \theta_2]$, $Q_2(\theta) > Q_1(\theta)$;

5. $\forall \theta \in [\theta_1, +\infty)$, $Q_1'(\theta) < 0$;

6. The function Q_2 has a unique global maximum at $\theta_1 < \theta^* < \theta_2$, i.e. $Q'(\theta^* + \zeta)\zeta < 0, \forall \zeta \neq 0$ s.t. $\zeta \in (-\infty, \theta_2 - \theta^*]$.

We can then state the following qualitative observations.

(a) Under the above conditions, it is clear that the time scale separation applies as in Section 3 : if, at some time, the trajectory is not in the vicinity of Q, it will quickly converge to this set. Thus we can consider, as illustrated by the simulations, that the trajectories are sequences of alternative fast jumps and quasi-static motions. Furthermore *if the parameter a is chosen sufficiently small*, the quasi-static trajectories along Q_2 converge to a small neighborhood of the optimal steady-state.

(b) But the simulations also show that, *if the parameter a is too small*, the trajectories on Q_1 may be stuck at the local maximum corresponding to the bifurcation point. Furthermore, when stuck on Q_1, condition (5) implies that θ_0 is automatically prevented to increase (in order to approach θ^*) since climbing along Q_1 is enforced by the ES control algorithm.

(c) Hence, although it is necessary to keep the parameter a rather small, it may also be necessary to increase a to pass through the bifurcation point and force a jump from Q_1 to Q_2 as in Fig.7. But, unfortunately, if a is too large, a cyclic behaviour as in Fig.9 is also possible.

The set-valued averaging analysis presented below gives a technical justification of the fact that increasing a may lead to passing through the bifurcation point. The definition of the averaged system makes use of the notion of Aumann integral in order to capture the complex trajectories that can occur in $[\theta_1, \theta_2]$.

As in Section 3, we introduce the change of coordinates $\tilde{\theta} = \theta_0 - \theta^*$ and the change of time scale $\sigma = \omega t$. But here, the $\tilde{\theta}$-dynamics become a *differential inclusion* (see e.g. [4, Chap.3]):

$$\frac{d\tilde{\theta}}{d\sigma} \in kQ(\theta^* + \tilde{\theta} + a\sin\sigma)a\sin\sigma. \tag{11}$$

where the right hand side is a set-valued 2π-periodic function. Then the average of system (11) is defined as the differential inclusion

$$\frac{d\theta_{av}}{d\sigma} \in kaf_{av}(a, \theta_{av}) \tag{12}$$

with $f_{av}(\sigma, \theta_{av})$ being the set-valued function defined as

$$f_{av}(a, \theta_{av}) \triangleq \frac{1}{2\pi}\int_0^{2\pi} Q(\theta^* + \theta_{av} + a\sin\sigma)\sin\sigma d\sigma$$

whith an Aumann integral on the right hand side (see [2]). (Given a set-valued map $F(.)$, the Aumann integral of F is defined as

$$\int F(s)ds \triangleq \left\{\int f(s)ds : f \in \Phi\right\}$$

where Φ is the set of integrals of all measurable selections from F.)

Let us now define the following single-valued function $Q_0(\theta)$ which is a selection from $Q(\theta)$:

$$Q_0(\theta) = \begin{cases} Q_1(\theta) & \theta_2 < \theta < +\infty \\ Q_2(\theta) & -\infty < \theta \leqslant \theta_2 \end{cases}.$$

Then we can write:

$$f_{av}(a, \theta_{av}) = \hat{f}_{av}(a, \theta_{av}) + g(a, \theta_{av})$$

with

$$\hat{f}_{av}(a, \theta_{av}) \triangleq \frac{1}{2\pi} \int_0^{2\pi} Q_0(\theta^* + \theta_{av} + a \sin\sigma) \sin\sigma d\sigma.$$

Under conditions (1)-(4), it can be shown that the set $g(a, \theta_{av})$ is upper bounded independently of a:

$$\max_{w \in g(a,\theta_{av})} |w| \leqslant M.$$

Then, a sufficient condition to avoid that the trajectory is stuck on Q_1 is obviously that $\theta_1 - \theta^*$ be not a fixed point of the average system :

$$0 \notin f(a, \theta_1 - \theta^*) = \hat{f}_{av}(a, \theta_1 - \theta^*) + g(a, \theta_1 - \theta^*)$$

We observe that $\hat{f}(0, \theta) = 0$ and therefore, by continuity, that we may have $0 \in f(a, \theta_1 - \theta^*)$ for small values of a. Hence it appears clearly that a sufficient condition for having $0 \notin f(a, \theta_1 - \theta^*)$ is that a be sufficiently large to get $|\hat{f}_{av}(a, \theta_1 - \theta^*)| > M$. This allows to understand why increasing the parameter a may prevent the trajectory to remain stuck on the lower equilibrium branch Q_1.

The "global" average behaviour captured by the Aumann integral includes all possible jumps between Q_1 and Q_2 branches that includes cyclic behaviours, such as the one given in Fig.9. These behaviours are observed in simulations for large values of dither amplitude a. However, as soon as the jump through the bifurcation point on Q_1 has occurred and the trajectory has converged to Q_2 (e.g. Fig.7), we can apply the classical "local" reasoning using the single valued average behaviour on Q_2 only that would be valid on a neighbourhood of Q_2 as long as the trajectory stays close to it. If the dither amplitude a is not too large, Q_2 will act as an invariant manifold for the average system and we can conclude using results of Tan et al. [11] that the ES controller will converge to the global maximum.

6 Conclusion

In conclusion, our analysis shows that global extremum seeking is feasible for systems with multi-valued discontinuous cost functions, albeit with competing requirements on the value of the dither amplitude parameter a. In order to avoid getting stuck in bifurcation points of Q_1, the dither amplitude needs to be sufficiently large and in order to avoid cyclic behaviours of Figure 9, the dither amplitude needs to be sufficiently small. A possible solution is to have a time varying amplitude of dither which is initially large and then is adaptively reduced. This solution that is reminiscent of simulated annealing was used for global ES in presence of local extrema in Tan et al. [12]. However, it is obvious that the sets Q_1, Q_2, the initial value of amplitude a(0) and its rate of change will have to satisfy restrictive conditions in order for this strategy to work.

An alternative is to choose a constant dither amplitude that is large enough to avoid getting stuck in the bifurcation point (item (b)) but small enough so that Q_2 is an invariant manifold for the (classical) local average (item (c)). Again a set of restrictive conditions will have to hold in order for this strategy to work and a loss of performance is to be expected as the larger amplitudes will lead to larger variations of the real trajectories around the desired maximum.

Obviously, the possible theoretical results that could be proved using the above arguments will be of limited use since our underlying assumption is that the model and the cost to optimize are not known to the control designer. Nevertheless, the insights that we obtained suggest that the practitioners of ES controllers should explore experimenting with the size of dither amplitudes as the performance gains may be tremendous and may lead to global extremum seeking.

References

[1] K.B. Ariyur and M. Krstic, Real-Time Optimization by Extremum-Seeking Control, Wiley, 2003

[2] R.J. Aumann, Integrals of set-valued functions, *Journal of Mathematical Analysis and Applications*, Vol.12(1), pp. 1-12, 1965.

[3] J.E. Bailey and D.F. Ollis, Biochemical Engineering Fundamentals - Second Edition, McGraw-Hill, 1986.

[4] F.H. Clarke, Optimization and nonsmooth analysis, Wiley, New-York, 1983.

[5] F. Jadot, G. Bastin and J.F. Van Impe, Optimal adaptive control of a bioprocess with yield-productivity conflict, *Journal of Biotechnology*, Vol. 65, pp. 61-68, 1998.

[6] N.I. Marcos, M. Guay and D. Dochain, Output feedback adaptive extremum seeking control of a continuous stirred tank bioreactor with Monod's kinetics, *Journal of Process Control*, Vol. 14, pp. 807-818, 2004.

[7] N.I. Marcos and M. Guay and D. Dochain and T. Zhang, Adaptive extremum seeking control of a continuous stirred tank bioreactor with Haldane's kinetics, *Journal of Process Control*, Vol. 14, pp. 317-328, 2004.

[8] J.M. Modak and H.C. Lim, Optimal mode of operation of bioreactor for fermentations processes, *Chemical Engineering Science* , Vol. 47(15/16), pp. 3869 - 3884, 1992.

[9] D. Sarkar and J.M. Modak, Pareto-optimal solutions for multi-objective optimization of fed-batch bioreactors using nondominated sorting genetic algorithms, *Chemical Engineering Science*, Vol. 60, pp. 481 - 492, 2005.

[10] K. Shimizu, A tutorial review on bioprocess systems engineering, *Computers and Chemical Engineering*, Vol. 20, pp. 915 - 941, 1996.

[11] Y. Tan, D. Nesic and I. Mareels, On non-local stability properties of extremum seeking control, *Automatica*, Vol. 42, pp. 889-903, 2006.

[12] Y. Tan, D. Nesic, I. Mareels, A. Astolfi, On global extremum seeking in the presence of local extrema, *Proceedings IEEE Conference on Decision and Control*, San Diego, CA, pp. 5663-5668, 2006.

[13] A.R. Teel, L. Moreau and D. Nesic, A unification of time-scale methods for systems with disturbances, *IEEE Transactions on Automatic Control*, Vol. 48, pp. 1526-1544, 2003.

[14] H-H. Wang, M. Krstic and G. Bastin, Optimizing bioreactors by extremum seeking, *International Journal of Adaptive Control and Signal Processing*, Vol. 13, pp. 651-669, 1999.

[15] T. Zhang, M. Guay and D. Dochain, Adaptive Extremum Seeking Control of Continuous Stirred-Tank Bioreactors, *AIChE Journal*, Vol. 49(1), pp. 113-123, 2003.